Nuclear Inst. and Methods in Physics Research, A 957 (2020) 163432

Contents lists available at ScienceDirect

Nuclear Inst. and Methods in Physics Research, A

journal homepage: www.elsevier.com/locate/nima

Technical Notes

Neutron measurements from the interaction of a thick Ta target with protons at different energies

Sabyasachi Paul [a], G.S. Sahoo [a], S.P. Tripathy [a,c,*], S.C. Sharma [b], D.S. Joshi [a], M.S. Kulkarni [a,c]

[a] Health Physics Division, Bhabha Atomic Research Centre, Mumbai 400 085, India
[b] Nuclear Physics Division, Bhabha Atomic Research Centre, Mumbai 400 085, India
[c] Homi Bhabha National Institute, Anushaktinagar, Mumbai 400 094, India

ARTICLE INFO

Keywords:
Neutron spectrometry
CR-39 detector
Yield from Ta target
Dose at different angles

ABSTRACT

Neutron dosimetry and spectrometry with a Ta target is of concern in an accelerator environment considering its enormous use in a proton accelerator. The Ta target has a unique advantage considering the generation of short half lived radionuclides upon interaction with protons. This advantage extends its use as the beam stopping material at various locations of an accelerator. However, this target has a varied range of reactions to produce neutrons and prompt gammas depending on proton energies. So in the present work, the neutron spectra were generated at various incident proton energies and neutron ambient dose equivalents were estimated close to the target projectile interaction at 90° with respect to the incident beam direction. A comparison of the spectral nature and doses were also done with measurements made by our earlier studies carried out at 0°. The comparison clearly showed that, apart from an increase in the low energy neutron yields at 90°, the overall yield distribution remains similar at both 0° and 90° angles with respect to the incoming beam direction. The ratio of the ambient neutron dose equivalent is found to reduce by a factor of 3–4 at 90° compared to 0° over the entire incident proton energy range. So, the dose equivalent ratio at two angles can be considered as independent of the incident projectile energy.

1. Introduction

In recent years, the particle accelerators are increasingly used as powerful tool in almost all fields of scientific research to industrial evolutions. Presently the energy as well as the particle flux in such accelerators is touching new heights and at the same time this brings out new radiological challenges for designers and operators. In such cases, with variation in the particle accelerator parameters, the interaction processes and the generation of the secondary particles differ significantly with particle type and energy [1]. In accelerator environments, the radiation nature is primarily pulsed and complex due to the presence of different types of target materials which interact with the primary particles and generates high energy photons and many other types of secondary particles [2]. Among those, neutrons possess the greatest challenge due to its significant radiological responses because of its multiple modes of interactions with the human body at different energy regimes, and also due to variable emission yields and spectra for different targets [3]. Secondly, the detection of neutrons and dosimetric quantification involves discrimination of neutron pulse from other interfering pulses. For detection of neutrons, a bulky moderation sphere becomes necessary for bringing the reaction generated fast neutrons to the thermal region for higher neutron interaction efficiency with the detector material. Along with the desired target projectile interactions in an accelerator, there exists possibility of interaction from the backing material of the target assembly or structural materials available in surroundings as well. For example, Ta is often used as a beam dump or as backing substrate for thin targets like Be or Li due to very low and short half-life activation products within the medium. Considering these applications of Ta in an accelerator environment, a detailed analysis of the neutron spectra and integral neutron yields at various incident particle energies is relevant for the radiological protection aspects.

In the present work, a thick Ta target was irradiated with different protons energies and the neutron yield was estimated using CR-39 detector. The proton energies were varied between 6 MeV to 20 MeV, as this energy range covers a dynamic range of secondary neutron generation reactions [4,5]. The measurements were carried out at 90° with respect the incoming beam direction to have a comparison with the results obtained from earlier studies at 0 deg [4]. The incident proton energies used in this work covers the emission neutron reactions from (p, n) to (p, 3n) in the entire proton energy regimes studied. For neutron detection in mixed radiation field with high energy photons, solid polymeric track detector, viz. CR-39 is specifically chosen to

* Corresponding author at: Health Physics Division, Bhabha Atomic Research Centre, Mumbai 400 085, India.
E-mail address: tripathy@barc.gov.in (S.P. Tripathy).

https://doi.org/10.1016/j.nima.2020.163432
Received 10 December 2019; Received in revised form 7 January 2020; Accepted 12 January 2020
Available online 15 January 2020
0168-9002/

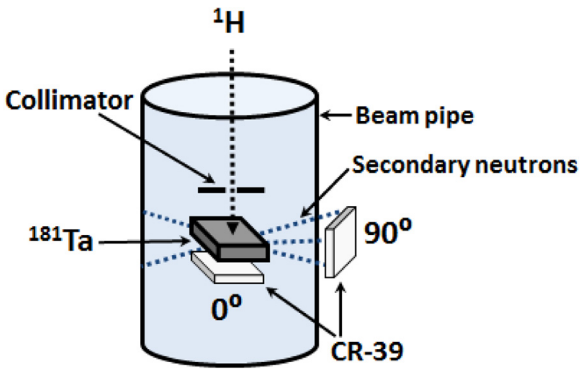

Fig. 1. Schematic of the proton irradiation geometry and detector locations.

estimate the neutron fluence through secondary recoil reactions within the detector. This detector is chemically classified as poly-allyl diglycol carbonate (PADC, $C_{12}H_{18}O_7$) and remains unresponsive to low linear energy transfer (LET) components like photons and electrons. Other advantages of these detectors are small size, permanent and cumulative mode of track registration, which allows its application even in a pulse radiation environment [6]. The small size of detectors allows the user to place it in any available geometry and location for radiation field estimation and the offline processing of these passive detectors does not require any other associated accessories during the irradiations. Latent tracks are formed within the detectors via recoil reactions with the neutrons and these latent tracks are further developed to microscopic dimensions using a suitable etching method [7,8]. From the track parameters, the particle fluence, neutron spectra and the dose rate were generated using an in-house image analyzing program autoTRAK_n [9–12]. The corresponding 0° measurements are reported elsewhere [4] and in the present work, we have referred those results for comparison of the neutron spectra, gross yields and ambient neutron dose equivalents with measured results at 90°. This was the primary objective of the study to analyze the angular dose distribution from the same reaction. In addition, it was of interest to verify the response of CR-39 detectors to neutron dose at different angles, because these are being widely used as personal neutron dosimeters, where the angular dependency is of major concern. These comparisons will give us an estimate of the yield profiles of neutron production ratio at different emission angles with increasing proton energies. This data would also be useful in implementing safe radiological practices in and around the accelerator facilities and for shielding calculations of upcoming proton accelerators.

2. Materials and methods

2.1. Irradiation

The irradiation of the CR-39 detector ($12 \times 12 \times 1.5$ mm^3, TASTRAK, UK) was carried out at 6M facility of the BARC-TIFR Pelletron accelerator facility [12], Mumbai at various proton energies between 6 to 20 MeV. For neutron generation, a 3.5 mm thick Ta plate is used as a target and the generated neutrons were captured using the CR-39 detectors through a permanent, cumulative mode of latent track registration. The detectors were kept at 90° with respect to the incoming beam direction at 5.1 cm from the Ta target and the schematic of the irradiation geometry is presented in Fig. 1. The total number of protons falling on the target was kept at 25.0 ± 0.1 μC for all incident proton energies, which was measured with a current integrator attached to the target with an average beam current of 70 nA. The maximum penetration depth of 20 MeV protons in a Ta target was estimated to be 608 μm [13] and the thickness of the target used (>5 times more than the particle range), was sufficient to completely stop the projectiles. In such case, all the latent tracks formed in the detector can be considered to be from the secondary neutrons generated from target projectile interactions and the possibility of direct proton tracks can be eliminated. After the proton irradiation, latent tracks formed were magnified with a suitable etching method (as explained below) and were counted on a microscope to obtain the necessary track parameters. During the track development process, a pristine detector was also processed and used for background correction.

2.2. Track development

The CR-39 detectors were developed using the conventional chemical etching technique (6.25 N NaOH at 70 °C for 6 h) for enlarging the latent tracks. Further the 2 dimensional (2D) track images were captured through a 5 MP camera attached to the optical microscope (Carl Zeiss). The images were taken in the transmission mode and the light intensity was adjusted to keep the central location of the tracks more luminous compared to the track boundaries. These images of 2D tracks were further processed with the in-house image analyzing program autoTRAK_n [9–12] to obtain the track parameters like track depth, angle of incidence, track size, etc. These parameters were then analyzed to obtain the neutron spectra for various incident proton energies.

2.3. Generation of Neutron spectra

The basic track geometry, the estimated particle grazing angle, track depths estimated using the in-house autoTRAK_n program were correlated with the recoil proton energy from the elastic scattering of the neutrons within the detectors. The track depth to recoil proton energy correlation was obtained from the stopping range calculations in the detector medium [13] and the energy dependent track to neutron response function [14] was used to estimate the neutron energy spectra. The neutron energy spectra were generated at 1 MeV bin width. The associated uncertainties at each bin widths were calculated based on the variation in the recoil track depths lying in the energy bin and the total number of available tracks per energy bin. For calculation purposes, these two set of information was randomly sampled using a Monte Carlo sampling technique to find out the statistical uncertainties following the parametric statistics at 95% confidence interval [10]. From the neutron energy spectra, the neutron ambient dose equivalent $H*(10)$ was estimated using the ICRP-74 [15] dose conversion coefficients per unit charge of incident protons in units of mSv μC^{-1}, for all incident proton energies. The background neutron spectrum was also obtained by processing the pristine detector using the same method, which was used for background correction.

3. Results and discussion

3.1. Analysis of neutron spectra at various proton energies

The study of the neutron spectra between 6–20 MeV proton energies at 90° with respect to the beam direction is obtained at a distance of 5.1 cm from the Ta target and the shapes of the neutron spectra were found to vary with incoming proton energy, mainly in the intermediate neutron energies. The total neutron yield increases with the increase in proton energy. The comparison of the neutron spectra at different proton energies with measurements carried out in this work and the reported values at 0° [4] is shown in Fig. 2. The comparisons are shown in three different figures with variable incoming proton energies. In Fig. 2(a), the neutron spectra obtained from 6 to 10 MeV are presented, which shows that, the peak energy of the neutron spectrum at 90° is shifting towards lower energies with respect to the measurements at 0°. In case of 90° measurements, the maximum yields were found in the energy bin up to 1 MeV and further the emission neutron yield reduced continuously with increasing energy. So, apart from the peak

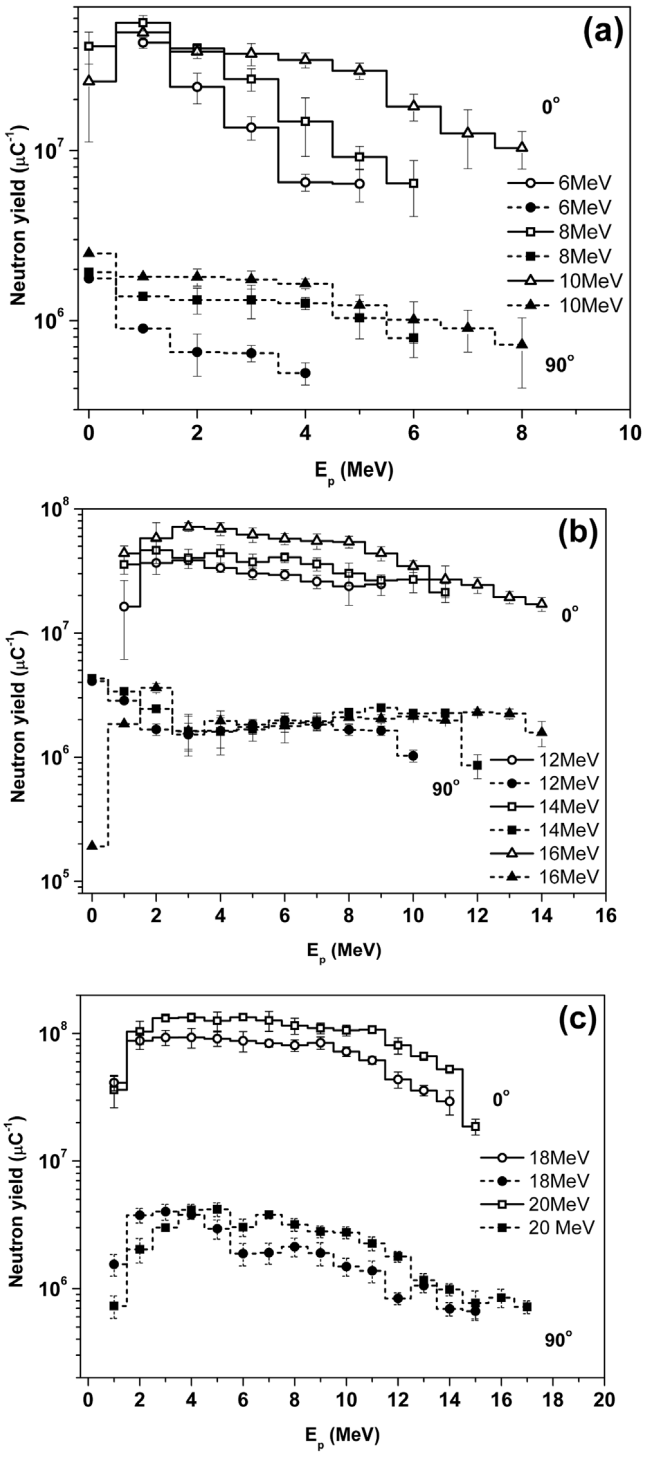

Fig. 2. Comparison of the neutron energy spectra from ^{1}H+Ta interaction at 0° [4] and 90° at different proton energies (a) 6–10 MeV (b) 12–16 MeV and (c) 18–20 MeV.

value, at all other emission energies, the spectral pattern follows a similar trend. The lower energy peak shifting can be attributed to the reduced neutron energy at 90° emissions compared to 0° emission spectra due to energy anisotropy in the lab frame from evaporation neutrons. The reduction in the yield is subjected to the higher flux at 0° and lesser target to detector distance compared to 90° measurements. For incident proton energy of 12–16 MeV, the yields at higher energy was found to remain almost constant over the entire emission energy range, as shown in Fig. 2(b). As can be seen in Fig. 2(b), the yields

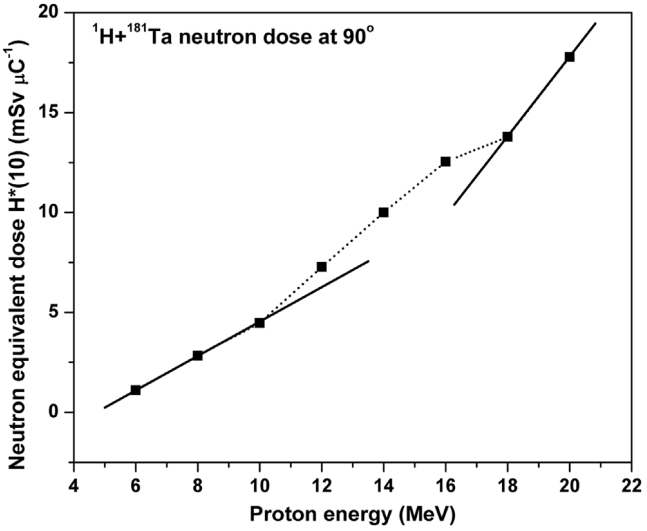

Fig. 3. The neutron ambient dose equivalent values for different proton energies at target to detector distance of 5.1 cm in the 90° direction with respect to the beam.

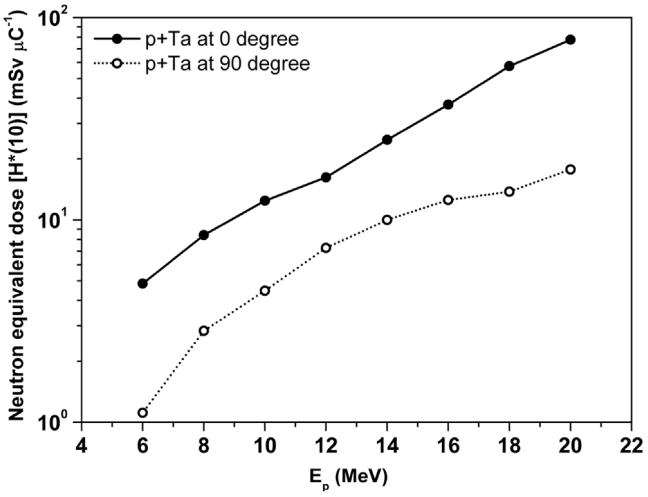

Fig. 4. Comparison of the neutron doses at 0° and 90° for a ^{1}H+ ^{181}Ta target at 5.1 cm (0° neutron dose measurements [4] are scaled at 5.1 cm).

at intermediate neutron energy between 4–8 MeV was found to have similar yields for all energies at 90° whereas at 0°, the emission yields were found to be decreasing for all incident energies. At higher proton energies of 18–20 MeV, as in Fig. 2(c), apart from the lower energy part of the measurement, the 90° measurements showed similar trend in the differential energy spectra compared to 0°. At lower neutron energy part, for 18 MeV protons, the neutron peak was found between 2–3 MeV whereas for 20 MeV protons, the peak was found to be between 3–4 MeV. These neutron spectra at various proton energies at two different emission angles will provide a better estimate of the ambient neutron dose equivalent based on energy dependent ICRP-74 dose conversion coefficient values discussed in the next section.

3.2. Estimation of neutron dose equivalent (H(10)) at various proton energies*

The neutron dose equivalent H*(10) were obtained by folding the measured neutron energy spectra with corresponding energy dependent ICRP-74 dose conversion coefficients [15]. The dose values obtained for the ^{1}H+Ta reaction at 90° at a target to detector distance of 5.1 cm is shown in Fig. 3. As can be seen in Fig. 3, with increase in incoming

Table 1
Total neutron yield and dose comparison at 0° [4] at 1.8 cm and 90° at 5.1 cm from target for different proton energies.

Energy (MeV)	Measurements at 0° [4]		Measurements at 90°	
	Yield (μC^{-1})	Dose (mSv μC^{-1})	Yield (μC^{-1})	Dose (mSv μC^{-1})
6	$9.34 \times 10^7 \pm 1.23 \times 10^7$	38.79	$4.46 \times 10^6 \pm 3.26 \times 10^5$	1.11
8	$2.04 \times 10^8 \pm 3.33 \times 10^7$	67.33	$9.06 \times 10^6 \pm 1.07 \times 10^6$	2.83
10	$2.67 \times 10^8 \pm 4.78 \times 10^7$	99.57	$1.34 \times 10^7 \pm 1.56 \times 10^6$	4.47
12	$3.10 \times 10^8 \pm 5.31 \times 10^7$	129.85	$2.17 \times 10^7 \pm 1.90 \times 10^6$	7.27
14	$4.63 \times 10^8 \pm 8.23 \times 10^7$	199.14	$2.47 \times 10^7 \pm 2.99 \times 10^6$	10.40
16	$6.88 \times 10^8 \pm 1.02 \times 10^8$	296.95	$2.90 \times 10^7 \pm 3.48 \times 10^6$	12.55
18	$1.06 \times 10^9 \pm 1.40 \times 10^8$	460.31	$3.16 \times 10^7 \pm 5.18 \times 10^6$	13.79
20	$1.45 \times 10^9 \pm 1.65 \times 10^8$	622.19	$3.99 \times 10^7 \pm 5.13 \times 10^6$	17.78

proton energy the neutron doses are increasing. However, it follows increasing slopes at different energy regimes. This variation in slopes can be attributed to the opening of multiple (p, xn) reaction channels at increasing proton energies. In the proton energy range from 6 to 10 MeV, the neutron yield increases in a linear pattern from 1.1 mSv μC^{-1} at 6 MeV to 4.5 mSv μC^{-1} at 10 MeV. At these proton energies up to 8 MeV, only the (p, n) reaction contributes to the total neutron yield from the target projectile interaction [4], so only one type of secondary neutron production reaction leads to the yields at this energy range. Beyond 8 MeV, the initiation of (p, 2n) reaction occurs but in the present measurement at 10 MeV dose contribution from (p, 2n) reaction was found to be insignificant at 90°. At energies from 12 to 16 MeV, the dose values showed an increase in the neutron yield compared to that in lower energy regime. This can be correlated to the contributions from (p, 2n) along with (p, n) reactions. At energies beyond 16 MeV, the reaction cross-section for both (p, n) and (p, 2n) reduces and the (p, 3n) reaction starts to contribute in the neutron yield largely, leading to a sharp increase in neutron dose. A comparison of the total neutron dose equivalent values obtained at 0° and 90° are presented in Fig. 4. During the 0° irradiation, the target to detector distance was kept 1.8 cm and the corresponding doses are reported in [4]. To get a comparison between the 0° and 90° doses at the same location, the 0° dose values were scaled down using the standard inverse square law at 5.1 cm and presented in Fig. 4. The figure shows that, the neutron ambient dose equivalent varies with a factor of 3–4 times between 0° to 90° measurements at all incident proton energies. So, it can be considered as the ratio between the doses at the two different emission angles. This ratio remains almost constant at all the incoming proton energies. However, the gross yields are reduced at 90° measurements due to anisotropic neutron yields at the lab frame of reference assuming an evaporation type of emission (see Table 1).

4. Conclusion

In the present work, the neutron spectra at 90° were reported for incident proton energies between 6–20 MeV and the corresponding ambient neutron dose equivalents were estimated. The incident proton energies used for this study covers the neutron emission from (p, n) to (p, 3n) reactions on a thick Ta target. The neutron yield increases with increase in the incoming particle energy and the effective yields showed different increasing slopes at different projectile energy regions due to combined effect of secondary neutron emission reactions at different projectile energy regime. A comparison of the neutron spectra and estimated doses obtained between 0° and 90° measurements were also carried out. Due to different detector to target distances at measurements in two angles, a simple comparison was not possible. In such case, the measured doses at respective locations for both angles need to be scaled at a common distance for a meaningful comparison of the ambient doses. Finally, upon scaling the neutron ambient doses, comparisons scaled at the same target to detector distance revealed that the ratio between 0° to 90° measurements for proton bombardment on a thick Ta target are almost independent of energy and the factor lies around the value of 3.5. Some small variation between the 0° and 90° measurements in the neutron spectra was observed. Primarily at 90° measurements, the contribution from the lower energy neutrons was found to be higher than the corresponding 0° measurements. The total neutron yield at a target to detector distance of 5.1 cm for proton energies between 6–20 MeV was found to vary between 4.46×10^6 to 3.99×10^7 neutrons per μC of incident proton charge. The estimated ambient dose equivalent values were found to vary from 1.11 to 17.78 mSv μC^{-1} for 6 and 20 MeV protons respectively. This indicates a reduction of neutron $H*(10)$ value nearly 3.5 times at 90° compared to the values at 0° measurements for a thick Ta target.

Declaration of competing interest

The authors declare that they have no known competing financial interests or personal relationships that could have appeared to influence the work reported in this paper.

CRediT authorship contribution statement

Sabyasachi Paul: Investigation, Methodology, Data curation, Software, Validation, Writing - original draft. **G.S. Sahoo:** Investigation, Formal analysis. **S.P. Tripathy:** Conceptualization, Investigation, Data curation, Writing - review & editing. **S.C. Sharma:** Resources, Supervision. **D.S. Joshi:** Project administration, Investigation. **M.S. Kulkarni:** Project administration, Supervision.

Acknowledgments

The authors thank the staffs of Pelletron Linac Accelerator Facility for their constant support during the experiment. Authors sincerely acknowledge Dr. T. Bandyopadhyay, former Head, ARSS for his guidance during the work. Authors are grateful to Shri R. M. Suresh Babu, Associate Director, Health, Safety & Environment Group, BARC for their support and inspiration in carrying out these studies.

References

[1] P.K. Sarkar, Neutron dosimetry in the particle accelerator environment, Radiat. Meas. 45 (2010) 1476–1483.
[2] S. Agosteo, Overview of novel techniques for radiation protection and dosimetry, Radiat. Meas. 45 (2010) 1171–1177.
[3] T. Nakamura, Neutron energy spectra produced from thick targets by light-mass heavy ions, Nucl. Instrum. Methods Phys. Res. A 240 (1985) 207–215.
[4] Sabyasachi Paul, G.S. Sahoo, S.P. Tripathy, S.C. Sharma, D.S. Joshi, T. Bandyopadhyay, Measurement of thick target neutron yield from the reaction (p $+^{181}$Ta) with projectiles in the range of 6–20 MeV, Nucl. Instrum. Methods Phys. Res. A 880 (2018) 75–79.
[5] Experimental nuclear reaction data (EXFOR), database version of 2019-10-07, NNDC BNL, 2019, Available at https://www.nndc.bnl.gov/exfor/exfor.htm. (Accessed 10 December 2019).
[6] S.P. Tripathy, Neutron spectrometry and dosimetry using CR-39 detectors, Solid State Phenom. 238 (2015) 1–15.
[7] S.A. Durrani, R.K. Bull, Solid State Nuclear Track Detection, Pergamon Press, Oxford, 1987.

[8] S.P. Tripathy, R.V. Kolekar, C. Sunil, P.K. Sarkar, K.K. Dwivedi, D.N. Sharma, Microwave-induced chemical etching (MCE): A fast etching technique for the solid polymeric track detectors (SPTD), 612, 2010, pp. 421–426.

[9] S. Paul, S.P. Tripathy, P.K. Sarkar, Analysis of 3-dimentional track parameters from 2-dimensional images of etched tracks in solid polymeric track detectors, Nucl. Instrum. Methods Phys. Res. A 690 (2012) 58–67.

[10] S. Paul, S.P. Tripathy, G.S. Sahoo, T. Bandyopadhyay, P.K. Sarkar, Measurement of fast neutron spectrum using CR-39 detectors and a new image analysis program (autoTRAK_n), Nucl. Instrum. Methods Phys. Res. A 729 (2013) 444–450.

[11] S.P. Tripathy, S. Paul, G.S. Sahoo, V. Suman, C. Sunil, D.S. Joshi, T. Bandyopadhyay, Measurement of fast neutron spectra from the interaction of 20 MeV protons with thick Be and C targets using CR-39 detector, Nucl. Instrum. Methods Phys. Res. 318 (2014) 237–240.

[12] S. Paul, G.S. Sahoo, S.P. Tripathy, S.C. Sharma, Ramjilal, N.G. Ninawe, C. Sunil, A.K. Gupta, T. Bandyopadhyay, Measurement of neutron spectra generated from bombardment of 4 to 24 MeV protons on a thick 9Be target and estimation of neutron yields, Rev. Sci. Instrum. 85 (2014) 063501.

[13] J.F. Ziegler, M.D. Ziegler, J.P. Biersack, SRIM – The stopping and range of ions in matter, Nucl. Instrum. Methods Phys. Res. 268 (2010) 1818–1823.

[14] S. Mayer, M. Boschung, H. Hoedlmoser, T. Buchillier, C. Bailat, B. Bitterli, Intercomparison of the response of different photon and neutron detectors around a spent fuel cask, Radiat. Meas. 47 (2012) 634–639.

[15] Conversion coefficients for use in radiological protection against external radiation. ICRP publication 74, Ann. ICRP 26 (3–4) (1996).